2011 American Control Conference
on O'Farrell Street, San Francisco, CA, USA
June 29 - July 01, 2011

An experimental comparative study of different second order sliding mode algorithms on a mechatronic actuator

Fayez S. Ahmed, Salah Laghrouche and Mohammed El Bagdouri
Laboratoire SET, Université de Technologie de Belfort-Montbéliard, Belfort, France

Abstract- ***This paper presents experimental results of practical implementation of three higher -order sliding-mode control algorithms. The considered algorithms are applied to the position control of an engine air path mechatronic actuator. This actuator is used to control the swirl air entering the cylinders of a diesel engine. Three output-feedback second order sliding-mode controllers have been designed and tested on the actuator. The most effective strategies have been tested for robustness in varying temperature and load conditions. The experimental results show the effectiveness and robustness of the control techniques.***

I. Introduction

In modern vehicles, combustion engines and their associated systems depend upon mechatronic actuators controlled by an ECU [1]. The engine air path is an important component of the engine system, consisting of the air inlet and exhaust mechanisms and related actuators[2, 3]. Mechatronic actuators allow faster response times and accuracy in transient conditions [2, 4, 5]. However, they are difficult to control because of nonlinearities coming from several sources such as highly varying engine temperature, external load perturbations, and aero-load dynamics [2, 5, 6, 7, 8]. Friction between mechanical parts causes stick-slip, and part wear [6, 7, 9]. These nonlinearities lead to uncertainty in actuator parameters due to variations in electrical and mechanical properties

The air path performance is a major factor in vehicle emissions and pollution control. With the worldwide increasing strictness in pollution laws, (e.g. Euro 5 (2010) and Euro 6 (2015)), contemporary research is focused on robust control over air path actuators, reliable under uncertain conditions [5, 8, 10, 11]. Song and Byun [4] have considered time-delay control with reference varying model for actuator positioning. Scattolini and Rossi [5, 8] have worked on modeling, identification and robust control of throttle bodies using position, velocity and current controllers. Along with Contreras *et al* [6], their work is in the direction of friction identification and compensation. Lee *et al* [10] and Pavkovic *et al* [10], have considered PID variants, using adaptive PID control and standard PID with friction and limp-home compensation respectively. These contributions are significant in actuator control. However, they lack the aspect of robustness to parametric uncertainty.

Sliding mode control (SMC) [11] is considered to be one of the most effective methods under uncertainty conditions [12-25]. Classical SMC suffers from chattering due to the high frequency discontinuous control [12, 13, 14, 15]. Higher order Sliding Mode Control (HOSMC) reduces chattering, by acting on a higher time derivative of the sliding variable instead of the first derivative [13, 14, 15, 16, 18, 19, 20]. Detailed work has been done on HOSMC by Bartolini, Levant, and Laghrouche [14, 15, 16].

In contemporary literature, sliding mode controllers and observers have been proposed for mechatronic actuators, resulting in robust control algorithms applicable to actuator control [13, 14, 15, 16, 17, 19, 23, 24, 28]. Pan *et al* [17], for example have considered first order SMC with a sliding mode observer for velocity and current measurement. Horn *et al* [23, 24] have successively used first and second order SMC in their works. Pisano *et al* have used higher order SMC in the output feedback control of marine actuators.

The objective of this paper is to address practical issues in implementation of Second Order Sliding mode control. The paper presents a performance comparison of three Second Order SMC algorithms on an air path actuator, using two types of sliding surfaces. The comparison has two purposes, firstly to evaluate the performance of the algorithms amongst themselves, and then to evaluate the sliding surfaces with respect to the algorithm performances. With the actuator subjected to parametric uncertainty by varying temperature and adding external perturbations, the algorithm performance has been considered in terms of time response, chattering and robustness.

The paper is divided in the following manner. Section two describes the motor and spring system modeling. Section 3 describes the modeling and identification of the LuGre friction model. Section 4 and 5 explain the second-order sliding mode theory controller design. Experimental results have been discussed in section 6. Some conclusions have been presented in section 7.

II. Actuator Model

In modern diesel engines, the swirl actuator is integrated in the air inlet manifold (figure 1). The manifold consists of two air ducts for each cylinder, one letting air directly into the cylinder, and the other allowing swirled air into the cylinder, the amount of which is controlled by the actuator.

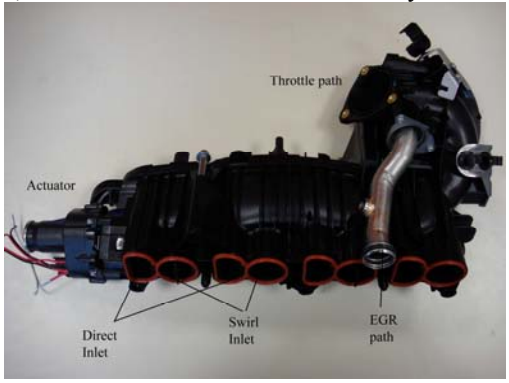

Figure 1: Air Inlet system of a modern diesel engine

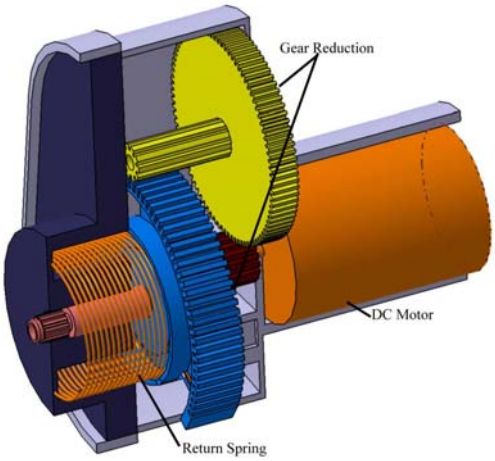

Figure 2: 3D cutaway drawing

As seen in figure 2, the actuator consists of a DC motor, a return spring and gearing. The significant number of mechanical parts results in friction and stick-slip, spring nonlinearities. Operational uncertainties (e.g. temperature) also make accurate control difficult. A detailed and physically motivated simulation model has been defined in [11, 30. The actuator can be modeled in the form of the following equations [5, 11, 17, 29, 30]:

$$V_a = i_a R_a + L_a \frac{di_a}{dt} + E_a \qquad (1)$$

$$J_{tot} \frac{d\omega}{dt} = T_m - T_{spr} - T_{pc} - T_f \qquad (2)$$

In (1), V_a is the armature voltage, i_a is the armature current, R_a is the motor coil resistance, L_a is the motor coil inductance. In general, the term $L_a\, di_a/dt$ can be neglected since the mechanical time constant is generally much greater than the electrical time constant [5, 6]. E_a is the motor back EMF and is defined as:

$$E_a = K_{em} r\omega = K_a \omega$$

Where, K_{em} is the motor electromagnetic constant, ω is the angular velocity of the actuator output shaft and r is the gear ratio. In (2), J_{tot} is the total moment of inertia of the system. The motor and spring torques can be defined by:

$$\left.\begin{aligned} T_m &= K_a i_a = K_a \left(\frac{V_a - K_a \omega}{R_a} \right) \\ T_{spr} &= K_{spr} \theta \end{aligned}\right\} \qquad (3)$$

K_{spr} is the spring constant and T_f is the friction force, (modeled in the next section). T_{pc} is the spring pre-compression torque. A detailed modeling of the dynamics has been presented in [11, 30], from where we can obtain the following dynamic model:

$$x_1 = \theta,\ x_2 = d\theta/dt,\ u = V_a$$

$$\dot{x}_1 = x_2$$

$$\dot{x}_2 = -\omega_n^2 . x_1 - 2\zeta\omega_n . x_2 - \frac{(T_{pc} + T_f)}{J_{tot}} + K\omega_n^2 u \qquad (4)$$

Where

$$\omega_n = \sqrt{\frac{K_{spr}}{J_{tot}}}, \zeta = \frac{K_a^2}{2R_a\sqrt{J_{tot} K_{spr}}}, K = \frac{K_a}{K_{spr} R_a}$$

In order to simplify writing, $\dot{x}_2$ can be expressed as

$$\dot{x}_1 = x_2$$

$$\dot{x}_2 = f(x_1, x_2) + g.u + \vartheta \qquad (5)$$

Where

$$f(x_1, x_2) = -\omega_n^2 . x_1 - 2\zeta\omega_n . x_2,\ g = K\omega_n^2,\ \vartheta = -\frac{(T_{pc} + T_f)}{J_{tot}}$$

It can be seen that the dynamic parameters depend heavily upon motor resistance, which changes with temperature. Exact identification of friction also, is a challenging task. Hence the actuator parameters can be uncertain in different operating conditions.

III. Friction

Friction is a natural force that exists between two surfaces in contact, moving relative to each other. It arises essentially from surface irregularities or asperities [7, 18]. The different phenomena associated with friction have been illustrated in figure 3 (for details, see [7].).

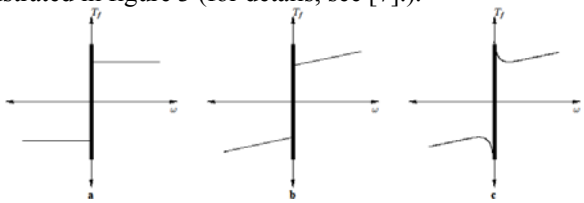
Figure 3: Friction Force (a) Static and Coulomb friction, (b) Viscous friction added, (c) Stribeck effect

The discontinuity induced in the system by static friction is especially hard to model and simulate on the computer [19]. Hence models, which have a dynamic response to the velocity of the system, are more effective for simulation, since they are continuous.

A. LuGre Friction Model

The LuGre Friction model considers asperities as elastic bristles instead [27]. Motion, according to this model occurs when the bristles start 'slipping'. It allows for the static friction to be modeled separately, and also incorporates Stribeck effect in the model [6, 7, 18, 27, 28]. The LuGre model has the following form

$$\left.\begin{aligned} T_f &= \sigma_o z + \sigma_1 \dot{z} + \sigma_2 \omega \\ \dot{z} &= \omega - \sigma_o \frac{|\omega|}{g(\omega)} z \end{aligned}\right\} \qquad (6)$$

Where z is the average deflection of the bristles before slipping, σ_o, σ_1 and σ_2i are stiffness, damping and viscous coefficients respectively [7, 18, 20]. $g(\omega)$ the Stribeck function is defined for ω_s as :

$$g(\omega) = T_c + (T_s - T_c) e^{(-\omega/|\omega_s|)^\alpha} \qquad (7)$$

DeWit has explained the identification process of the other parameters in detail in [27]. Practical identification on a similar actuator has been discussed in [30].

IV. Second-Order Sliding Mode

Let us consider an uncertain nonlinear system:

$$\dot{x} = f(x,t) + g(x,t)u$$

$$y = s(x,t) \qquad (8)$$

Where $x \in \mathrm{R}^n$ and $u \in \mathrm{R}$ is the input control and $s(x,t) \in \mathrm{R}$ is a measured smooth output-feedback function

(sliding variable). *f(x,t)* and *g(x,t)* are uncertain smooth functions. Let us establish two hypotheses, as follows:

H1. The relative degree ρ of the system with respect to *s* is constant and known and the zero dynamics are stable.

The 2nd order SMC approach allows the finite time stabilization to zero of the sliding variable *s* and $\dot{s}$ by defining a suitable control function *'u'*. Let us consider two sliding variables, S_1 and S_2. The system (8) has relative degrees ρ=2 and ρ=1 with S_1 and S_2 respectively. We obtain the following two distinct second order dynamics.

A. ρ=2

$$\dot{S}_1 = \frac{\partial S_1}{\partial t} + \frac{\partial S_1}{\partial x}\left[S_1\right]\left[f(x)+g(x)u\right], \text{ with } \frac{\partial}{\partial x}S_1(x,t)g(x)u = 0$$

$$\ddot{S}_1 = \frac{\partial^2 S_1}{\partial t^2} + \frac{\partial}{\partial x}\dot{S}_1(x,t)f(x) + \frac{\partial}{\partial x}\dot{S}_1(x,t)g(x)u$$
$$= \phi_A(x,t) + \gamma_A(x,t)u$$

B. ρ=1

$$\dot{S}_2 = \frac{\partial S_2}{\partial t} + \frac{\partial S_2}{\partial x}\left[S_2\right]\left[f(x)+g(x)u\right], \text{ with } \frac{\partial}{\partial x}S_2(x,t)g(x)u \neq 0$$

$$\ddot{S}_2 = \frac{\partial^2}{\partial t^2}S_2(x,t,u) + \frac{\partial}{\partial x}\dot{S}_2(x,t,u)\left[f(x)+g(x)u\right] + \frac{\partial}{\partial x}\dot{S}_2((x,t,u)\dot{u}(t)$$
$$= \phi_B(x,t,u) + \gamma_B(x,t,u)\dot{u}$$

H2. Functions $\varphi(.)$ and $\gamma(.)$ are bounded uncertain functions and the sign of control gain γ is strictly positive.

The fact that the uncertainty is bounded means that there are constants $K_m \in \mathrm{R}^{+*}$, $K_M \in \mathrm{R}^{+*}$, $C_o \in \mathrm{R}^{+}$, such that

$$0 < K_m < \gamma < K_M, \qquad |\phi| \le C_O$$

The second-order sliding-mode problem may be expressed in terms of the finite time stabilization problem of the following uncertain second-order system.

$$\dot{\xi}_1 = \xi_2$$
$$\dot{\xi}_2 = \varphi(.) + \gamma(.)v$$

then, cases *A* and *B* become:

$$A:\begin{cases}\phi(.)=\phi_A(x,t)\\ \gamma(.)=\gamma_A(x,t)\\ v(t)=u(t)\end{cases} \quad B:\begin{cases}\phi(.)=\phi_B(x,t,u)\\ \gamma(.)=\gamma_B(x,t,u)\\ v(t)=\dot{u}(t)\end{cases}$$

Where $\xi_x = S_x$, $\xi_x = \dot{S}_x$.

In the following sub-sections, we would present the algorithms for thecontrol laws *u(t)* and $\dot{u}(t)$. The constants C_0, K_M, and K_m are important in determining the parameters of the control laws, as would be presented in the next subsection.

A. Robust differentiator

The performance of the sliding-mode controller depends upon the exact derivative of the sliding variable *s* and hence requires robust differentiation. Levant [13] has proposed an exact finite time convergent differentiator [25] to combine with the feedback controller. For a function *x*, the differentiator has the form:

$$\dot{z}_o = -\lambda_2 L^{1/2}\left|z_o - x\right|\mathrm{sgn}(z_o - x) + z_1$$
$$\dot{z}_1 = -\lambda_1 L\,\mathrm{sgn}(z_1 - z_o)$$

Where z_o and z_1 are estimates of *x* and $\dot{x}$ respectively, and λ_1, λ_2 and *L* are strictly positive constants. These constants need to be evaluated empirically. Certain guiding values can however be found in Levant [13], along with a detailed discussion of the robustness.

B. Control algorithms

Our goal is to design a second-order sliding-mode controller with respect to the sliding variable *S,* i.e. to bring and hold the trajectories to the manifold defined by

$$S^2 = \left\{x \in X \middle| s(x,t) = \dot{s}(x,t) = 0\right\}$$

Many methods have been proposed to achieve this objective, in the works of Levant and Bartolini [13, 14, 15, 16, 19, 25].Three second-order sliding-mode algorithms have been taken into consideration in this study.

B.1. Twisting Algorithm

The twisting algorithm is based on adequate commutation of the control between two different values that allow the trajectories to converge towards origin in finite time [20]. This algorithm is defined by the following control law.

$$u = \begin{cases} -u & \text{if } |u| > u_{\max} \\ -\alpha_m\,\mathrm{sgn}(\xi_1) & \text{if } \xi_1\xi_2 \le 0 \text{ and } |u| \le u_{\max} \\ -\alpha_M\,\mathrm{sgn}(\xi_1) & \text{if } \xi_1\xi_2 > 0 \text{ and } |u| \le u_{\max} \end{cases}$$

Here u_{max} is the maximum limit value of control (in our case, input voltage) that can be physically applied, while α_M and α_m are strictly positive constants. They are bound by the following conditions which are sufficient to ensure finite time convergence to the sliding variable.

$$\begin{cases} 0 < \alpha_m < \alpha_M, & \alpha_m > \dfrac{C_O}{K_m} \\ K_m\alpha_M - C_O > K_M\alpha_m + C_O \end{cases}$$

B.2. Super-twisting algorithm

The super-twisting algorithm [23, 24] is limited to systems of relative degree 1 with respect to the sliding variable. It has the following form:

$$\dot{u}_1 = \begin{cases} -u & \text{if } |u| > u_{\max} \\ -\alpha\,\mathrm{sgn}(\xi_1) & \text{if } |u| \le u_{\max} \end{cases}$$

$$u_2 = -\phi\sqrt{|\xi_1|}\,\mathrm{sgn}(\xi_1)$$

$$u = u_1 + u_2$$

Where α and φ are strictly positive constants. The following conditions are imposed to ensure convergence

$$\alpha > \frac{C_o}{K_m}, \quad \phi^2 \ge \frac{4C_oK_M(\alpha + C_o)}{K_m^3(\alpha - C_o)}$$

B.3 Quasi-continuous second order controller

The quasi-continuous second order sliding mode controller [13] is a feedback function of s_1 and s_2 which is continuous everywhere except on the sliding manifold. It has the following form:

$$u = -\alpha\frac{\xi_2 + \sqrt{|\xi_1|}\,\mathrm{sgn}(\xi_1)}{|\xi_2| + \sqrt{|\xi_1|}}$$

Where α is a strictly positive constant. Unfortunately, there are no conditions and its value is found empirically.

V. Control Design

In this section, we will discuss the implementation of the algorithms. The aim is to design a robust control system

tracks a reference trajectory x_{ref} under parameter and load variations. Second-order sliding-mode approach requires two steps, selection of a sliding variable suitable for the control task, to design a control law that would make the variable and its first derivative converge to the sliding manifold, and then to select a control algorithm and tune its parameters. Two sliding variables have been studied in this paper, defined by S_1 and S_2.

Sliding variable S_1

The first sliding variable has the following form

$$S_1 = x_1 - x_{ref}$$

The system (4) has a relative degree ρ=2 with respect to this variable. In order to obtain the second-order control law we obtain the second derivative

$$\ddot{S}_1 = \left[-\omega_n^2 x_1 - 2\varsigma\omega_n x_2 - (T_{pc} + T_f)/J_{tot} + K\omega_n^2(u)\right] - \ddot{x}_{ref}$$

Considering equation (5), we can write

$$\ddot{S}_1 = f(x_1, x_2) + \vartheta + g.u - \ddot{x}_{ref} + \delta$$

where δ is a bounded parameter which accounts for parameter uncertainties, such as variations due to temperature, and external perturbations. The following control law would permit to linearize the system.

$$u = \left[(v - f(x_1, x_2) - \vartheta - \ddot{x}_{ref})/g\right]$$

This control will bring the following function to the sliding manifold

$$\ddot{S}_1 = v + \delta \qquad (9)$$

Sliding variable S_2

The second sliding variable has the form of Hurwitz polynomial

$$S_2 = \dot{e} + \lambda e\ ,\quad where\ \ e = x_1 - x_{ref}$$

The system (4) has a relative degree ρ=1 with respect to this variable. In order for it to converge on the sliding manifold, the second-order sliding mode control law can be found as

$$\dot{S}_2 = f(x_1, x_2, z) + \lambda\dot{e} + g.u - \ddot{x}_{ref}$$

$$\ddot{S}_2 = \dot{f}(x_1, x_2, z) + \lambda\left[f(x_1, x_2, z) + g.u\right] + g\dot{u} - (\lambda\ddot{x}_{ref} + \dddot{x}_{ref})$$

$$\ddot{S}_2 = \psi(x_1, x_2, z, u) + g\dot{u} - (\lambda\ddot{x}_{ref} + \dddot{x}_{ref}) + \hat{\delta}$$

The following control law would permit to linearize the system.

$$\dot{u} = (\hat{v} - \psi(x_1, x_2, u) + (\ddot{x}_{ref} + \dddot{x}_{ref}))/g$$

This control will converge the following function to the sliding manifold

$$\ddot{S}_2 = \hat{v} + \hat{\delta} \qquad (10)$$

The disturbances δ and $\hat{\delta}$ are uncertain but bounded. The problem of second order sliding mode control now is equivalent to the stabilization of equations (9) and (10) to zero in finite time. This task will be accomplished by applying discontinuous control on *'v'* using the three algorithms presented in the last section. The actuator physical parameters have been experimentally found out using the methods given in [5, 11, 30], the values are given in table 1. Detailed discussion on finding bounding constants and controller parameters has been presented in [29]. Here, we have presented only the controller parameters, the values are given in table 2.

VI. Experiments and Results

The control strategies were implemented in LabView, using the National Instruments CompactRio system. The actuator was mounted on a test bench equipped with a high resolution dynamometer and encoder. This test bench has a temperature controlled chamber using which actuators can be tested in different temperature conditions. An external hysteresis brake allows torque variation.

Quantity	Unit	Value
Gear Ratio r	-	27.5
Electromagnetic coefficient K_{em}	mN.m/A	13.82
Spring constant K_{spr}	mN.m/rad	60.88
Winding resistance R_a	Ω	3.35
Moment of inertia J_{tot}	Kg.m^2	9.65X10^{-7}
Spring pre-compression T_{pc}	mN.m	119.4
Static friction T_s	mN.m	51.2
Coulomb friction T_c	mN.m	47.13
Stribeck velocity ω_s	Rad/sec	0.002
LuGre stiffness coefficient σ_o	-	2800
LuGre damping coefficient σ_1	-	53
LuGre viscous coefficient σ_2	-	0.012

Table 1: Actuator parameters

Algorithm	Parameter	Value
Twisting	α_m	10000000
	α_M	500000
Quasi-continuous	α	250
Super-twisting	α	5
	φ	15
Differentiator	λ_1	1.1
	λ_2	1.5
	L	260

Table 2: Controller parameters

All the controllers except the super-twisting were tested on both the variables described in the previous section. The super-twisting algorithm was implemented only on variable S_2 since it is the only one with respect to which, the system has relative degree of 1.

A. Test Trajectory

The reference trajectory used to test the control laws is shown in figure 4. This trajectory is an industrial bench mark, in fact used by a certain manufacturer of EGR valves for performance evaluation of their systems

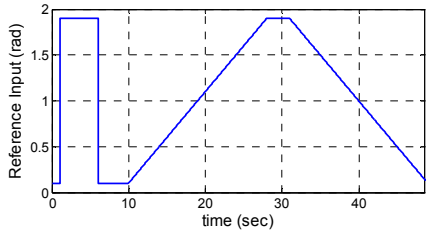

Figure 4: Reference Trajectory

B. Test Results:

In all the figures, the result of variable S_1 is presented in blue and the result of variable S_2 is presented in red.

B.1. Sliding variable S_1:

Variable S_1 proved to be prone to chattering, as can be seen in figure 5 and 6. Both the twisting algorithm and the quasi-continuous algorithm show a chattering level as high as 0.1 radians.

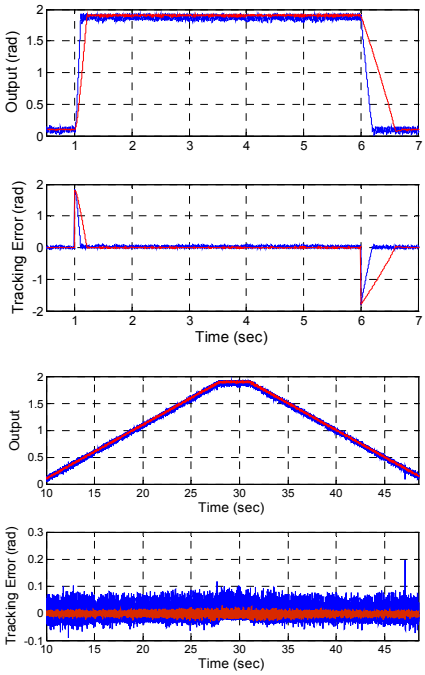

Figure 5: Twisting Algorithm

B.2. Sliding variable S_2:

All the controllers perform well on S_2., with λ=100. As can be seen in figure 5, the chattering in the twisting algorithm was reduced drastically with the use of this surface, however the time response became worse, increasing from 300msec to 600msec. The quasi-continuous controller saw improvement in both chattering level and time response. On S_2, the quasi-continuous algorithm achieved 120 msec. The best performance was shown by the super-twisting algorithm which achieved a time response of 100msec with a chattering level in the order of 5 mrad.

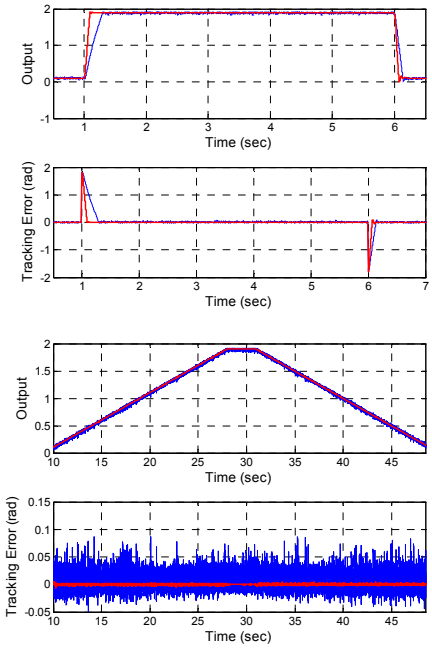

Figure 6: Quasi-continuous second order controller algorithm

Further tests were performed on the quasi-continuous controller and on the super-twisting algorithm, in order to verify their robustness. The first test was performed by applying a an external torque of 25mNm, using the brake. As can be seen in figures 8a and 9a, which show the normal response in blue and the perturbed response in red, the controllers adjusted their output to compensate for the external torque, without any noticeable deflection from the trajectory. In the next test, temperature was varied from 20°C to 100°C. Again both the controllers managed to maintain their performance characteristics.

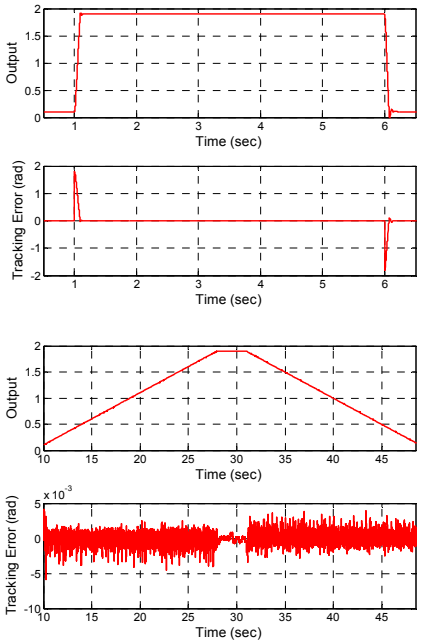

Figure 7: Super-twisting algorithm

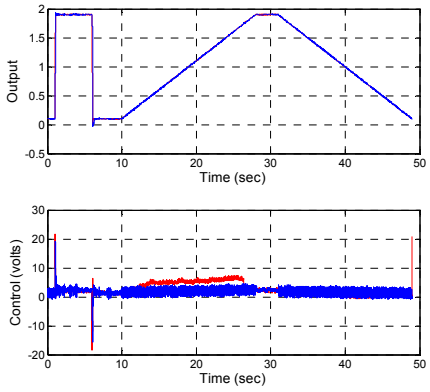

(a)

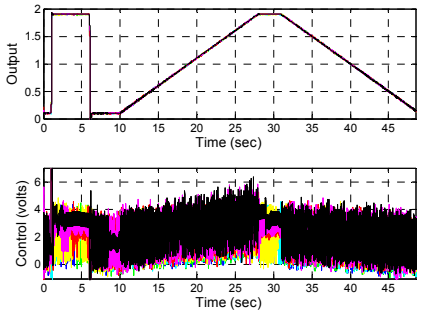

(b)

Figure 8: Quasi-controller (a) external perturbation (b) varying temperature

VII. Conclusion

In this study, three second order sliding mode controllers with different sliding surfaces were used to control a mechatronic swirl actuator. Control strategies were simulated and their parameters determined. In general, second order SMC, proved to be robust against actuator parametric uncertainty, as claimed. All controllers performed well in tracking. The chattering phenomenon was reduced significantly using the quasi-continuous controller and was almost negligible when the super-twisting algorithm was applied. With respect to surfaces, surface S_2 (Hurwitz polynomial) was better than surface S_1. The quasi continuous controller and the super twisting controller on S_2 proved their worth in terms of robustness under temperature variations and external perturbations

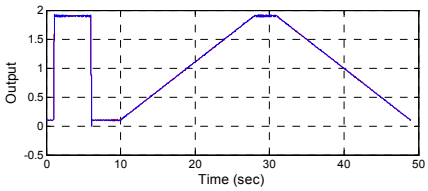

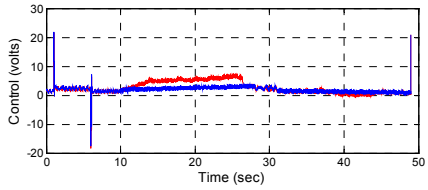

(a)

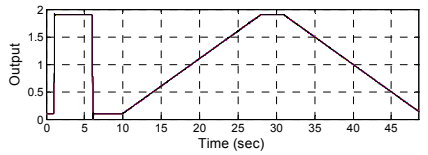

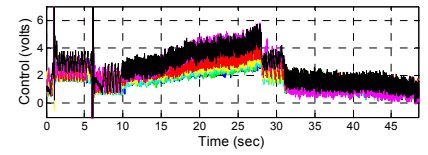

(b)

Figure 9: Super-twisting algorithm (a) external perturbation (b) varying temperature

References

1. R. Isermann, R. Schwarz, S. Stolzl, "Fault-tolerant drive-by-wire systems" *Control System Magazine 22* 22-24 (2002).
2. R. Hoseinnezhad, A. Hadiashar, Missing Data Compensation for Safety-Critical Components in a Drive-by-Wire System", *IEEE Trans. Vehicular Technology Vol.* 54 (July 2005).
3. M. Bertoluzzo, G. Buja, "Design of a Safety-Critical Drive-By-Wire System Using FlexCAN" *SAE International* (2005).
4. J. B. Song, K. S. Byun, "Throttle Actuator Control System for Vehicle Traction Control" *Mechatronics 9* 477-495 (1999).
5. R. Scattolini, C. Siviero, M. Mazzucco, S. Ricci, L. Poggio and C. Rossi, "Modeling and Identification of an Electromechanical Internal Combustion Engine Throttle Body" *Control Eng. Practice* Vol. 5. No.9. pp. 1253-1259 (1997).
6. F. Contreras, I. P. Quiroz, C. C. deWit, "Further Results on Modeling and Identification of an Electronic Throttle Body" *10th* -MED *Conf. Control and Automation* (July, 2002).
7. H. Olsson, K.J. Åström, C. Canudas de Wit., M. Gäfvert, P. Lischinsky, "Friction Models and Friction Compensation" *European Journal of Control* 4(3) (1998).
8. C. Rossi, A. Tilli, A. Tonielli "Robust Control of a Throttle Body for Drive by Wire Operation of Automotive Engines", *Control Engineering Practice Vol.* 9, *1235-1244*, (2001).
9. D. Lee, J. Allan, H. A. Thompson, S. Bennett "PID control for a distributed system with a smart actuator", *IEEE Trans. Ind. Electronics, Vol. 54, No. 1* (2007).
10. D. Pavkovic, J. Deur, M. Jansznn, "Adaptive Control of Automotive electronic Throttle" *Conl Engineering Practice* 121-136 (2006).
11. F. S. Ahmed, S. Laghrouche, M. El Bagdouri, "Modeling and identification of a mechatronic exhaust gas recirculation actuator of an internal combustion engine", *IEEE American Control Conference* (July, 2010).
12. V. I. Utkin, "Sliding Modes in Optimization and Control Problems", *New York: Springer Verlag* (1992).
13. A. Levant, "Quasi-Continuous High-Order Sliding-Mode Controllers", *IEEE Trans. Automatic control, Vol. 50 (*2005).
14. G. Bartolini, A. Ferrara, E. Usai, V. I. Utkin, "On Multi-Input Chattering-Free Second-Order Sliding-Mode Control", *IEEE Trans. Automatic Control, Vol. 45, No. 9,* (2000).
15. G. Bartolini, E. Punta, T. Zolezzi, "Regular simplex method and chattering elimination for nonlinear sliding mode control of uncertain systems", *IEEE Conf. Decision and Control,* (2007).
16. A. Levant, "Homogeneity approach to higher-order slidng-mode design", *Automatica 41, pp* 823-830 (2005).
17. Y. Pan, U. Ozguner, O. H. Dagci, "Variable-Structure Control of Electronic Throttle Valve", *IEEE Trans. Indusrial Electronics Vol. 55, No. 11* (2008).
18. S. Laghrouche, F. Plestan, A. Glumineau, R. Boisliveau, "Robust second order sliding mode control of a permanent magnet synchronous motor", *Proc. American Control Conference* (2003).
19. G. Bartolini, A. Ferrara, E. Usai, "Chattering avoidance by second order sliding mode control", *IEEE Trans. Automat. Control Vol. 43 No. 2* (1998).
20. A. Levant, "Sliding order and sliding accuracy in sliding mode control", *International Journal of Control Vol. 58 No. 6* (1993).
21. A. Pisano, E. Usai, "Output-feedback control of an undervater vehicle prototype by higher-order sliding modes", *Automatica 40, pp.* 1525-1531, (2004).
22. S. Laghrouche, F. Plestan, A. Glumineau, "Higher order sliding mode control based on integral sliding mode", *Automatica Vol. 43 pp. 531-537* (2007).
23. M. Reichhartinger, M. Horn, "Application of Higher Order Sliding-Mode Concepts to a Throttle for Gasoline engines", *IEEE Trans. Industrial Electronics, Vol. 56 No. 9* (2009).
24. M. Horn, A. Hofer, M. Reichhartinger, "Control of an Electronic Throttle Valve based on Concepts of Sliding-Mode Control", *17th IEEE International Conf. Control Applications* (2008).
25. Levant, "Higher-order sliding modes, differentiation and output-feedback control", *Int. J. Control, Vol. 46, No. 9* (2001).
26. D. Karnopp, "Computer Simulation of Stick-Slip Friction in Mechanical Dynamic Systems**"** *ASME Journal of Dynamic Systems, Measurement and Control, 107, 100-103* (1985).
27. C. C. de Wit, H. Olsson, k. J. Astrom, P. Lischinsky, "A new model for control of systems with friction", *IEEE trans. Automatic control, vol. 40, No. 3* (1995).
28. Z. Wenjing, "Parameter identification of Lugre Friction Model in Servo System Based on Improved Particle Swarm Optimization Algoritm", *Proc. 26th Chinese Control Conference* 135-139 (2007).
29. F. S. Ahmed, S. Laghrouche, M. El Bagdouri, "Second Order Sliding Mode based Output Feedback Control of an Engine Air Path Actuator in presence of uncertainties", *Conference on Control and Fault Tolerant Systems* (September, 2010).
30. F. S. Ahmed, S. Laghrouche, M. El Bagdouri, "Nonlinear modeling of pancake DC Limited angle torque motor based on LuGre model", *Vehicle Power and Propulsion Conference* (September, 2010).